Epitaxial growth of Bi thin films on Ge(1 1 1)

AUTHOR(S):

Hatta, Shinichiro; Ohtsubo, Yoshiyuki; Miyamoto, Sanae; Okuyama, Hiroshi; Aruga, Tetsuya

CITATION:

Hatta, Shinichiro ...[et al]. Epitaxial growth of Bi thin films on Ge(1 1 1). Applied Surface Science 2009, 256(4): 1252-1256

ISSUE DATE:

2009-11-30

Epitaxial growth of Bi thin films on Ge(111)

Shinichiro Hatta [a,b,*] Yoshiyuki Ohtsubo [a] Sanae Miyamoto [a]

Hiroshi Okuyama [a] Tetsuya Aruga [a,b,**]

[a] *Department of Chemistry, Graduate School of Science, Kyoto University, Kyoto 606-8502, Japan*

[b] *JST CREST, Saitama 332-0012, Japan*

Abstract

We investigated Bi thin film growth on Ge(111) by using low-energy electron diffraction (LEED) and scanning tunneling microscopy (STM). In the submonolayer regime, adsorbed Bi atoms form patches of the (2×1) structure. However, the structure does not grow to a long-range order. Following the formation of a (1×1) monolayer (ML) film, two-dimensional (110)-orientated Bi islands grow. The film orientation changes from (110) to (111) at 6–10 ML. The (110)-oriented Bi film shows a six-domain LEED pattern with missing spots, associated with a glide-line symmetry. The hexagonal (111) film at 14 ML has a lattice constant 2% smaller than bulk Bi(111).

Key words: Low-energy electron diffraction, scanning tunneling microscopy, thin film growth, Bismuth, Ge(111)

* Corresponding author. Tel.: +81-075-753-3977, Fax.: +81-075-753-4000.
**Corresponding author. Tel.: +81-075-753-3978, Fax.: +81-075-753-4000.
Email addresses: hatta@kuchem.kyoto-u.ac.jp (Shinichiro Hatta),
aruga@kuchem.kyoto-u.ac.jp (Tetsuya Aruga).

1 Introduction

Surfaces and thin films of bismuth have gained much interest in recent years. In contrast to semimetallic bulk Bi, the low-index surfaces of Bi, such as Bi(111), Bi(110) and Bi(001), are well metallic.[1,2] Here the Miller indices are given according to the rhombohedral lattice notation. The surface electronic structure of Bi is characterized by large spin splitting of surface states (several hundreds of meV) due to the spin-orbit coupling associated with the inversion asymmetry at surfaces. This type of spin splitting in two-dimensional electron systems is called the Rashba effect.[3] The extent of the observed spin splitting is much larger than that expected by a model for the two dimensional free electrons, where the magnitude of out-of-plane potential gradient dominates the splitting energy. The heavy core potential must also be taken into account such large spin splitting in the valence-band region. The Bi thin films on various substrates are interesting for the study of the Rashba-type spin splitting, because they have two different film/vacuum and film/substrate interfaces.

The growth and electronic structure of Bi thin films on Si(111)-(7×7) have been extensively investigated.[4–12] Thin films on (7×7) with the first wetting layer shows a phase transformation at a critical thickness of $5-6$ monolayers.[4] At the first stage, the Bi(110)-like film with a black-phosphorus-like structure grows with randomly-distributed in-plane orientations. When the thickness exceeds $\sim$6 ML, the out-of-plane orientation changes from (110) to(111) accompanying internal structure change to that of bulk Bi. The single-crystalline Bi(111) film grows epitaxially in the layer-by-layer mode. The electronic structure of the Bi(111) film shows the large Rashba-type spin splitting at metallic surface bands near $\bar{\Gamma}$, as observed for the Bi(111) surface.[8,10,12] On the

other hand, from $\bar{\Gamma}$ to $\bar{M}$, the band character changes to quantum-well states with the wavefunction spread over the film. The quantum-well states are not spin-polarized, but the splitting remains due to the equivalent interference at the surface and interface. This is confirmed by the band calculation with the freestanding (111) film. This result indicates a fairly weak electronic coupling at the interface of Bi and the Si substrate. A similar thin film growth is also observed on a different substrate of Bi/Si(111)-$(\sqrt{3} \times \sqrt{3})R30°$.[9] Unlike the growth on Si(111)-(7×7), the wetting layer is not formed. It is suggested that the internal structure of the Bi(110)-like film is not close to black phosphorus but to bulk Bi. Beside, the in-plane orientation of the Bi(110)-like film is closely related to that of Si(111). Above a critical thickness of ∼10 ML, the growth of the polycrystalline Bi(111) film was observed.

While Ge is semiconducting as Si, the bulk band gap of Ge (0.7 eV) is smaller than that of Si (1.1 eV). Therefore the stronger interaction is expected between the Bi thin film and the Ge substrate. In this work, we studied the growth of Bi thin films on Ge(111) by using low-energy electron diffraction (LEED) and scanning tunneling microscopy (STM). In the submonolayer regime, we find a Bi-induced superstructure with a (2×1) periodicity. The structure does not grow to a long-range-ordered structure, and a (1×1) phase is formed at 1 ML. Above 2 ML, Bi(110)-like and, subsequently, Bi(111) films appear as the coverage increases. The in-plane orientations of both films are closely related to that of Ge(111). The sharp and three-fold Bi(111) (1×1) LEED pattern indicates the growth of nearly-single-crystallin films, as on Si(111)-(7×7).

2 Experimental

LEED and STM experiments were performed in two different ultrahigh vacuum chambers with a base pressure of $\sim 1 \times 10^{-10}$ Torr. We used a standard four-grid LEED optics and a variable-temperature STM (Oxford Instruments). All STM images were taken in the constant-current mode with electrochemically-etched tungsten tips. The n-type Ge(111) wafer ($\rho \sim 0.1 - 1\Omega$·cm) was cleaned by cycles of Ar ion sputtering at 700–800 eV and annealing at 900 K by direct current heating. Bi was deposited from an alumina crucible heated by tungsten wire loop on to Ge(111) at 120, 300 and 350 K. The most part of the data shown here was obtained from the sample prepared by the deposition at 300 K followed by annealing at $\sim$ 400 K for 1 min. Hereafter Bi coverages are given in MLs with 1 ML defined as the atom density of the Ge(111) surface. We assumed 1 ML as a coverage when a well-contrasted (1×1) LEED pattern was observed (Fig. 2(c)).

The bulk Bi rhombohedral lattice is defined by a lattice constant of 4.75 Å and an angle of 57.1°. Two atoms of a basis (1 and 5 in Fig. 1(a)) are separated by 5.52 Å along [111]. The atom pairs of 2–5, 3–5 and 4–5 have the nearest-neighbor distance of 3.05 Å. These bonds have a significant covalent character. A (110) atomic plane is defined as a plane including the atoms of 2, 4, 7 and 8. Because the atom 5 is only 0.14 Å below this plane, the unit cell of the (110) layer are often identified with two atoms as shown in Fig. 1(b). The pseudosquare lattice has a dimension of 4.54×4.75 Å^2. A (111) atomic plane is defined as a plane including the atoms of 2, 3 and 4. The lattice constant of the hexagonal (111) layer is 4.54 Å. Because the bond between two (111) layers with the nearest-neighbor distance is strong, the (111) surface is terminated

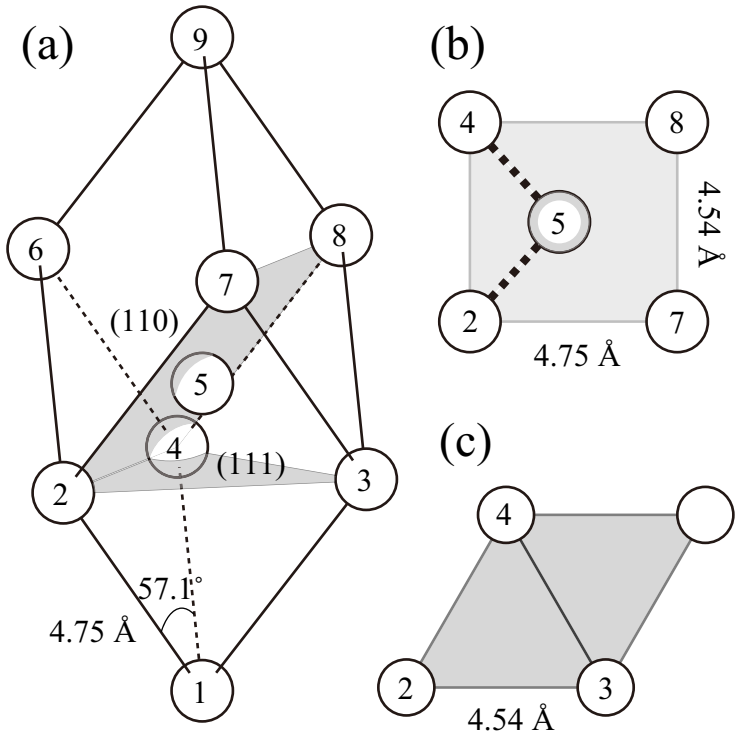

Fig. 1. (a)Schematic picture of the rhombohedral lattice of bulk Bi. (b)The pseudosquare Bi(110) plane. The bold dashed lines represent the bonds with the nearest-neighbor distance. (c)The hexagonal Bi(111) plane.

by the bilayer of (111) atomic planes.[14]

3 Results and discussion

Figure 2 shows the observed LEED patterns at various Bi coverages (0, 0.45, 1.0, 4.5, 6.5 and 14.5 ML). The clean Ge(111) surface shows a sharp $c(2 \times 8)$ patten, as shown in Fig. 2(a). The $c(2\times8)$ quarter-order spots disappear at the Bi coverage below 0.3 ML. Annealing of the Bi-covered surface above 400 K causes the $(\sqrt{3}\times\sqrt{3})R30°$ structure.[13] On the other hand, no LEED pattern was observed from the sample kept at 120 K.

Figure 3(a) shows an STM image at a very low coverage ($\Theta \leq 0.05$ ML).

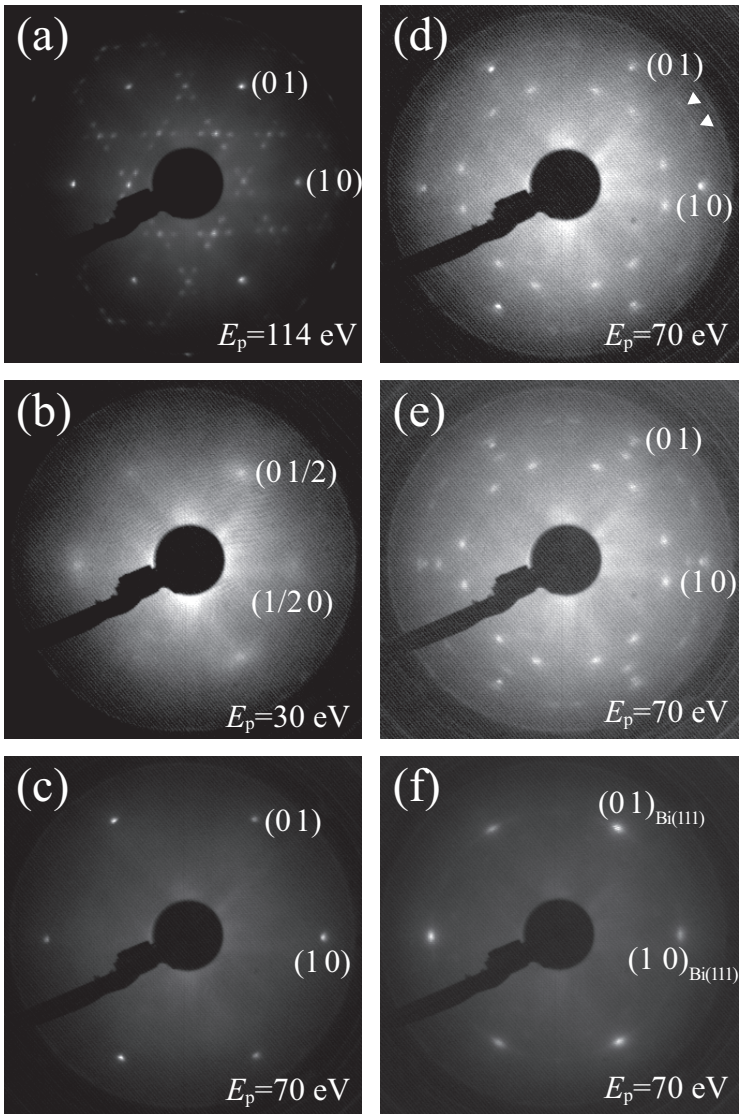

Fig. 2. (a)The LEED pattern of the clean Ge(111)-$c(2 \times 8)$ surface. (b)–(f) LEED patterns at the Bi coverage of 0.45, 1.0, 4.5, 6.5 and 14.5 ML, respectively. All the patterns are taken at room temperature.

The major part of the surface is still covered with the $c(2 \times 8)$ structure. Bi-induced features are seen as bright protrusions. While a single protrusion is rare (absent in Fig. 3(a)), dimers and tetramers are often found. Because the atomic radius (1.6 Å) of Bi is much larger than that (1.25 Å) of Ge, we postulate that the protrusions are adsorbed Bi atoms. The apparent height difference between the protrusions and Ge adatoms are only 0.85 ± 0.10 Å.

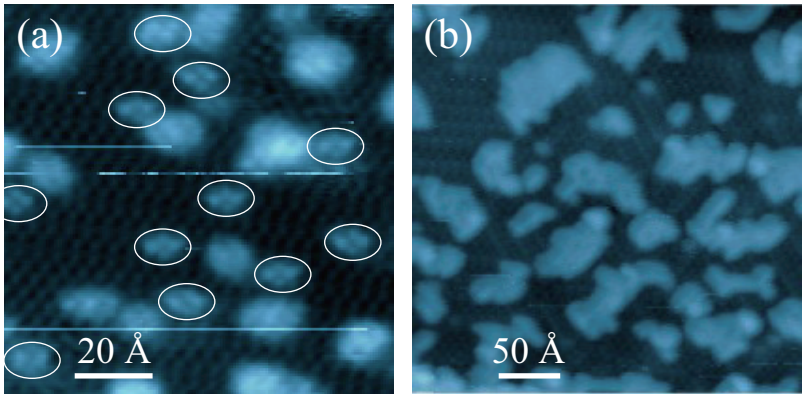

Fig. 3. (a) The STM images at $\Theta \leq 0.05$ ML ($V_s = 1.8$ V, $I_t = 0.2$ nA). The ellipsoids indicate the tetramers of the bright protrusions. (b) The STM images at ~ 0.2 ML ($V_s = -0.8$, $I_t = 0.80$ nA).

Therefore, it seems that Ge adatoms of the $c(2 \times 8)$ structure are replaced with Bi atoms.

With increasing coverage, the clusters grow to two-dimensional islands, as shown in Fig. 3(b). Each island grows separately and the remaining area is still covered with Ge adatoms. On these islands, weak stripe features are observed. The corrugation amplitude perpendicular to the stripes is at most 0.1 Å. The distance of 7 Å between the stripes corresponds to $\times 2$ periodicity along $\langle 1\bar{1}0 \rangle$ on Ge(111). The LEED pattern near this coverage shows half-order spots as shown in Fig. 2(b), while the spots must also have some contribution of the remnant $c(2 \times 8)$ structure.

The observed stripe feature seems to resemble the STM image of the Sb/Ge(111)-(2×1) structure.[15] The coverage of the (2×1) structure is suggested to be 1 ML. It is suggested that Sb atoms reside near atop sites of the bulk-truncated Ge(111) surface and form the zigzag (Seiwatz) chains, where the neighboring Sb rows approach toward one another. For Bi/Ge(111), however, because Bi has a covalent radius larger than Sb, the tendency toward the formation of the

Seiwatz chains is weakened compared to the case of Sb. Indeed, the half-order LEED spots become weak above 0.5 ML, and a new (1×1) phase is formed at 1 ML. The observed (1×1) LEED pattern is sharp and well contrasted as shown in Fig. 2(c).

With increasing coverage above 1 ML, the background intensity around the (00) LEED spot gradually becomes high. When the coverage reaches 2 ML, new spots appear. Figure 2(d) shows a LEED pattern at 4.5 ML, where 12 spots inside the Ge(111) (1×1) spots are located on a circle with a radius of 1.31 Å^{-1}, and 24 weak spots at $\sim$ 1.9 Å^{-1} just outside the Ge(111) (1×1) spots . The intensity of these spots is maximized at around 6 ML.

Figure 4(a) shows a large-scale STM image at 6 ML. The most part of the surface is covered with two-dimensional Bi islands with the size of 300–500 Å. The observed step height is evaluated to be 3.4$\pm$0.3 Å(see the inset of Fig. 4(a)), which roughly corresponds to the interlayer distance of bulk Bi(110) (3.28 Å). The islands have an average height of $\sim$10 Bi(110) layers. Figure 4(b) shows a high-resolution STM image taken at the island top. The atomic protrusions configure a pseudosquare lattice with the unit cell of 4.6×4.8 Å^2. The zigzag-chain feature is consistent with the nearest-neighbor atomic rows in the (110) plane of bulk Bi (Fig. 1(b)). Two atoms in a Bi(110) unit cell have a small height difference of 0.14 Å in bulk and 0.18 Å on the surface.[16] Lower Bi atoms are probably located on the darker corners of the zigzag chains.

We now review the LEED pattern of Fig. 2(c) on the basis of the STM observation. The distance of 1.31 Å^{-1} between the inner spots and (00) spot corresponds to 4.78 Å for a rectangular lattice. This length is in good agreement with the longer lattice constant on Bi(110). We suggest a schematic

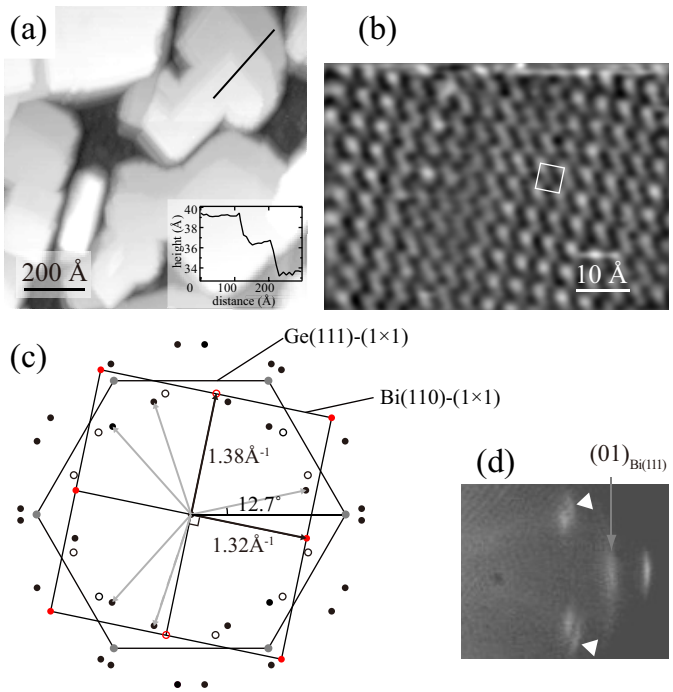

Fig. 4. (a) The large-scale STM images at $\sim$ 6 ML ($V_s = -1.0$ V, $I_t = 0.2$ nA). The inset shows the line profile taken along the solid line. (b) The atomically-resolved STM images taken on a Bi(110)-like island ($V_s = -3.5$ mV, $I_t = 1.0$ nA). (c) Schematic of the LEED pattern of the 6-domain Bi(110)-like surface. (d) The LEED pattern at 35 eV from the sample prepared by Bi deposition on the substrate at $\sim$ 350 K. The LEED pattern was taken at 150 K.

LEED pattern of Fig. 4(c), where filled circles represent the observed spots and open circles invisible spots in Figs. 2(d) and (e). The distance between the (00) spot and the invisible spots are 1.38 Å^{-1} corresponding to the shorter lattice constant of Bi(110) (4.57 Å). The primitive vectors of six domains, related by three-fold symmetry and a mirror plane along $\langle 11\bar{2} \rangle$ on Ge(111), reproduce the observed 24 spots outside the Ge(111) (1×1) spots. The long side of the pseudosquare unit cell is tilted at $\pm 12.7^\circ$ from $\langle 11\bar{2} \rangle$.

The missing spots in LEED can be ascribed to a glide-line symmetry along

the short side of a Bi(110) unit cell. The glide-line symmetry is realized if two atoms in a unit cell are located at the same height. While an STM image is sensitive to the local electron density relevant to the valence states, LEED electrons are scattered by ion cores. Therefore, if the height difference of the Bi atoms is negligibly small, the observed LEED pattern is explained with the glide-line symmetry. Another possible explanation is the interference of electrons from adjoining local domains with the inverted bond configuration. It is found near the center of Fig. 4(b) that the bright corner is switched on the opposite side of a zigzag chain. The static structural fluctuation is probably due to the lattice mismatch between Ge(111) and Bi(110)-like islands.

On the other hand, we found that the LEED pattern from Bi(110)-like islands slightly depends on the condition of the sample preparation. Figure 4(d) is a part of the LEED pattern from the sample prepared by the Bi deposition of 6 ML at 350 K. Spots corresponding to 4.57 Å are shown, as indicated by triangles. A spot of the Bi(111) film, which appears at higher coverages in the case of the room temperature deposition, are also found. These spots are broad and background intensity is high, compared to the LEED pattern of Fig. 2(e). It is expected that annealing during the deposition promotes the growth of higher islands with a smaller lateral dimension. The island shape may be related to the atomic structure and the order on the island top.

Comparing the Bi(110)-like film on Ge(111) with that on Si(111)-(7×7),[4,7] we found that the LEED patterns are quite different. For the Bi(110)-like film on the 7×7 surface, the ring pattern is observed, due to the random distribution of the in-plane orientation. This indicates a weak interaction between the Si(111) substrate and the film. The film has a black-phosphorus structure resulting from pairing of Bi(110)-like layers. The bilayer structure causes the

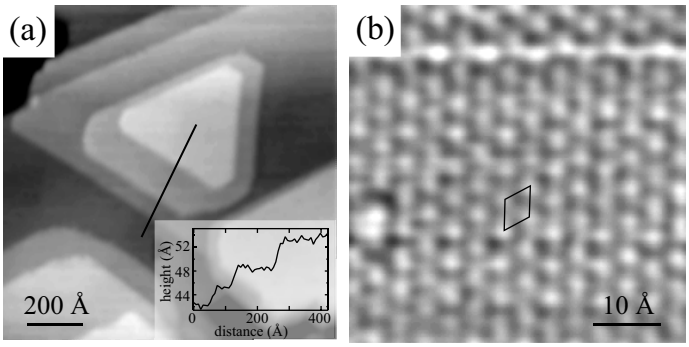

Fig. 5. (a) The large-scale STM images at $\sim$ 10 ML ($V_s = -2.0$ V, $I_t = 0.2$ nA). The inset shows the line profile taken along the solid line. (b) The atomically-resolved STM images taken on a Bi(111) film ($V_s = -4.5$ mV, $I_t = 0.6$ nA).

stability of the even-number-layer films. On the other hand, for the Bi(110)-like film on Ge(111), the crystal axes of the six domains are strongly aligned along the specific direction of the Ge(111) substrate. Besides, the observed single-layer steps on the islands indicate that the interior structure of the islands is close to that of bulk Bi rather than of black phosphorus. These results are similar to the Bi(110)-like film on Bi/Si(111)-$(\sqrt{3} \times \sqrt{3})R30°$.[9].

Above 6 ML, new six spots appear just inside the Ge(111) (1×1) spots. With increasing coverage, the Bi(110)-like and Ge(111) (1×1) spots are gradually weakened, and instead, the new spots becomes dominant. Figure 1(f) shows a LEED pattern at 14.5 ML, where the background intensity is as low as the monolayer film at 1 ML (Fig. 1(c)), indicating improvement of the surface flatness. The distance between the new and (00) spots is 1.63 Å^{-1}. For a hexagonal lattice, this corresponds to a lattice constant of 4.45 Å. This value is 2% smaller than that of bulk Bi(111) (4.53 Å). Figure 5(a) shows a large-scale STM image at 10 ML. The surface is covered with the Bi film. The film surface shows hexagonal atomic arrangement as shown in Fig. 5(b). The lattice constant is 4.5 Å, which is in good agreement with the LEED observation. The

observed step height of 3.8±0.3 Å is close to the Bi(111) bilayer height of 3.94 Å. Therefore, the atomic structure in the Bi(111) film is expected to be close to that of bulk Bi.

The LEED and STM observations show the transformation of the Bi film orientation from (110) to (111) depending on the coverage. While this behavior of the Bi thin film on Ge(111) is roughly the same as observed on Si(111)-(7×7) and Bi/Si(111)-$(\sqrt{3} \times \sqrt{3})R30°$, a critical thickness of the orientation change on Ge(111) is not clear and the LEED patterns of the two type of films are observed together over a wide coverage range of $6 - 10$ ML. This probably reflects a wide distribution of the island height compared to the film on Si(111). The in-plane orientation of the Bi(111) film on Ge(111) is highly ordered as that on Si(111)-(7×7). For the Bi(111) film on Si(111)-(7×7), a commensurate relation of $a_{7\times7} = 6a_{\mathrm{Bi(111)}}$ was suggested as an important factor to grow the single-crystalline Bi(111) film. The spot-profile LEED observation showed that the (7×7) periodicity is maintained below the Bi wetting layer. On the other hand, our LEED observation on Bi/Ge(111) showed that the Ge(111)-$c(2 \times 8)$ reconstruction is completely disturbed and only a (1×1) periodicity exists before the growth of the Bi(110)-like film. While a quasi-commensurate relation between the Ge(111) and Bi(111) is found as $9a_{\mathrm{Ge(111)}} = 8a_{\mathrm{Bi(111)}}$, such a commensurability seems to be no longer strict.

4 Summary

We have studied the growth of Bi thin films on the Ge(111) surface up to 14 ML. The (2×1) structure was found below 1 ML and does not grow to a long-range-ordered phase. For multilayer Bi films, the out-of-plane orientation

change from (110) to (111) was observed as on the Si(111) substrate. The in-plane orientations of the Bi(110)-like and Bi(111) films are highly ordered to Ge(111). This indicates that the film/substrate interaction on Bi/Ge(111) is stronger than that on Bi/Si(111).

Acknowledgements

The authors acknowledge the support by the Global COE Program "Integrated Materials Science" (No. B-09).

References

[1] Yu. M. Koroteev, G. Bihlmayer, J. E. Gayone, E. V. Chulkov, S. Blügel, P. M. Echenique, and Ph, Hofmann, Phys. Rev. Lett. **93** (2004) 046403.

[2] Ph. Hofmann, Prog. Surf. Sci. **81** (2006) 191.

[3] E. I. Rashba, Sov. Phys. Sol. St. **2**, 1109 (1960); Y. A. Bychkov and E. I. Rashba, JETP Lett. **39**, 78 (1984).

[4] T. Nagao, J. T. Sadowski, M. Saito, S. Yaginuma, Y. Fujikawa, T. Kogure, T. Ohta, Y. Hasegawa, S. Hasegawa, and T. Sakurai, Phys. Rev. Lett. **93** (2004) 105501.

[5] M. Kammler, and M. H. Hoegen, Surf. Sci. **576** (2005) 56.

[6] T. Nagao, S. Yaginuma, M. Saito, T. Kogure, J.T. Sadowski, T. Ohno, S. Hasegawa, and T. Sakurai, Surf. Sci. **590** (2005) L247.

[7] J. T. Sadowski, T. Nagao, S. Yaginuma, Y. Fujikawa, T. Sakurai, A. Oreshkin, M. Saito, and T. Ohno, J. Appl. Phys. **99** (2006) 014904.

[8] T. Hirahara, T. Nagao, I. Matsuda, G. Bihlmayer, E. V. Chulkov, Yu. M. Koroteev, P. M. Echenique, M. Saito, and S. Hasegawa, Phys. Rev. Lett. **97** (2006) 146803.

[9] S. Yaginuma, T. Nagao, J. T. Sadowski, M. Saito, K. Nagaoka, Y. Fujikawa, T. Sakurai, and T. Nakayama, Surf. Sci. **601** (2007) 3593.

[10] T. Hirahara, K. Miyamoto, I. Matsuda, T. Kadono, A. Kimura, T. Nagao, G. Bihlmayer, E. V. Chulkov, S. Qiao, K. Shimada, H. Namatame, M. Taniguchi, and S. Hasegawa, Phys. Rev. B **76** (2007) 153305.

[11] S. Yaginuma, K. Nagaoka, T. Nagao, G. Bihlmayer, Yu. M. Koroteev, E. V. Chulkov, and T. Nakayama, J. Phys. Soc. Jpn **77** (2008) 014701.

[12] T. Hirahara, K. Miyamoto, A. Kimura, Y. Niinuma, G. Bihlmayer, E. V. Chulkov, T. Nagao, I. Matsuda, S. Qiao, K. Shimada, H. Namatame, M. Taniguchi, and S. Hasegawa, New J. Phys. **10** (2008) 083038.

[13] K. J. Wan, W. K. Ford, G. J. Lapeyre, and J. C. Hermanson, Phys. Rev. B **44** (1991) 6500.

[14] H. Mönig, J. Sun, Yu. M. Koroteev, G. Bihlmayer, J. Wells, E. V. Chulkov, K. Pohl, and Ph. Hofmann, Phys. Rev. B **72** (2005) 085410.

[15] M. Kuzmin, P. Laukkanen, R.E. Perälä, M. Ahola-Tuomi, I.J. Väyrynen, Surf. Sci. **601** (2007) 837.

[16] J. Sun, A. Mikkelsen, M. Fuglsang Jensen, M. Koroteev, G. Bihlmayer, E. V. Chulkov, D. L. Adams, Ph. Hofmann, and K. Pohl, Phys. Rev. B **74** (2006) 245406.

[17] Yu. M. Koroteev, G. Bihlmayer, E. V. Chulkov, and S. Blügel, Phys. Rev. B **77** (2008) 045428.